Effect of stretching on the sub-T_g phenylene-ring dynamics of polycarbonate by neutron scattering

Silvia Arrese-Igor,[1] Olatz Mitxelena,[2] Arantxa Arbe,[1] Angel Alegría,[1,2] Juan Colmenero,[1,2,3] and Bernhard Frick[4]
[1]*Centro de Física de Materiales (CSIC-UPV/EHU), Apartado 1072, 20080 San Sebastián, Spain*
[2]*Departamento de Física de Materiales UPV/EHU, Apartado 1072, 20080 San Sebastián, Spain*
[3]*Donostia International Physics Center, Apartado 1072, 20080 San Sebastián, Spain*
[4]*Institut Laue-Langevin, Boîte Postale 156, 38042 Grenoble Cedex 9, France*
(Revised manuscript received 8 April 2008; published 12 August 2008)

We have investigated the effect of cold drawing on the motion of phenylene rings in bisphenol-A polycarbonate by neutron scattering. The intensity scattered by isotropic and stretched polycarbonate is different, the quasielastic broadening being larger for the isotropic sample. This difference can be well accounted for by considering that preferentially oriented rings in the stretched polymer have their motion sterically hindered. The extent of the effect of stretching on the phenylene-ring motion obtained from this neutron-scattering investigation is in good agreement with that obtained when studying the effect of cold drawing on the γ relaxation by dielectric spectroscopy.

DOI: 10.1103/PhysRevE.78.021801 PACS number(s): 36.20.Ey, 28.20.Cz

I. INTRODUCTION

The secondary relaxation of polycarbonate (PC) and other related engineering thermoplastics has been extensively investigated over the past decades because this process is believed to be directly related to the mechanical properties of polymers. Incidentally or intentionally, some degree of orientation or anisotropy is developed within polymers during their processing. Therefore, it is of great importance, both academic and technological, to investigate and understand the possible effects of orientation and anisotropy on the local molecular motions involved in secondary relaxations. Strictly speaking, secondary relaxations are those dynamic processes observed by spectroscopic conventional techniques like dielectric (DS) or mechanical spectroscopy. These techniques allow a good characterization of the shape and characteristic frequency of secondary relaxations in a broad frequency range (from $\sim 10^{-3}$ to $\sim 10^{9}$ Hz). However, these measurements do not provide microscopic spatial information of the motions involved. Therefore, some technique allowing the study and characterization of the motions at a molecular level is highly desirable.

The study of secondary γ relaxation of cold stretched PC by DS reveals that the intensities of the various components of the relaxation are affected by stretching to a different extent. In this work we aim to provide a molecular interpretation of the decrease of the different dielectric relaxation components in stretched PC by studying the phenylene-ring (PR) dynamics of stretched and isotropic PC by neutron scattering (NS), a technique which provides microscopic spatial information.

II. PHENYLENE-RING MOTIONS AND γ RELAXATION

The molecular motions of PRs within PC below its glass transition temperature (T_g=420 K) were first studied by nuclear magnetic resonance (NMR). The H^2 NMR of samples with deuterated PRs shows that PRs perform π-flip motion around the C1C4 axis superimposed by angle fluctuations that reach a root-mean-square amplitude of $\pm 35°$ at 380 K [1]. After cold drawing (draw ratio λ=1.7), motional restrictions on PRs equivalent to a temperature shift of 10 K have been reported also by H^2 NMR [2]. On the other hand, application of high hydrostatic pressure leads to an even more marked arrest of the motion of PRs seen by NMR [3].

Very recently quasielastic neutron-scattering techniques have been used to investigate the PR dynamics in polyethersulfone and several bisphenol-A (BPA) containing thermoplastics including PC [4–7]. The fact that hydrogen's incoherent scattering cross section is much larger than that of any other atom typically present in polymers allows one to selectively follow the motion of hydrogen atoms within a sample. NS experiments on PC, BPA-polysulfone, BPA-poly(hydroxyether), and polyethersulfone with different selective deuterations confirm the presence of PR π-flip motions with characteristics that change only slightly from polymer to polymer. The mean characteristic times obtained by this technique agree very well with those previously obtained by NMR for the same motion. By the combination of backscattering and time-of-flight NS techniques, it was also possible to infer and characterize the presence of fast PR oscillations of increasing amplitude with temperature, resulting in them essentially being the same for all polymers. Interestingly, regardless of these similarities, at temperatures $\gtrsim$300 K, PC shows larger quasielastic intensity than the rest of the polymers investigated. This excess signal can be well accounted for by a ~3-Å jump of aromatic hydrogen atoms with characteristic times between the faster oscillation motion and the slower π flips.

The molecular dynamics simulations of Shih *et al.* and Fan *et al.* of PC report coupled motion for the PR and carbonate groups and a clear four-state map for the rotation angle between these two groups (angles between different states are between 74° and 106°) [8,9]. In contrast, the vectors representing different main chain segments merely vibrate around their equilibrium positions without any significant rotation or reorientation [9]. Inspired by these works and by the fact that the distance covered by an aromatic hydrogen atom under a 90° rotation is 3.04 Å, the additional ~3-Å jump of aromatic hydrogen atoms in PC has been

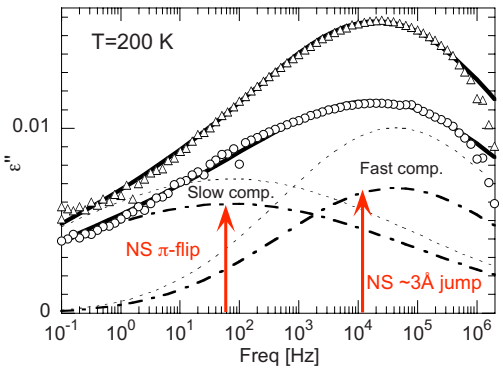

FIG. 1. (Color online) Imaginary part of the dielectric permittivity of an isotropic (triangles) and cold-drawn (circles) PC at 200 K. Solid lines represent the fit of the data. The two components are shown separately for isotropic and cold-drawn samples by the dotted and dash-dotted lines, respectively. Arrows indicate the mean characteristic times for a ~3-Å jump and π flips of PR extrapolated by NS. Modified from Ref. [14] with permission.

interpreted in a first approximation in terms of a ~90° rotation of PR linked to the motion of the adjacent carbonate group [6].

On the other hand, early and late dielectric relaxation investigations of the γ relaxation of PC evidence that it can be hardly associated with a single molecular motion as it presents several contributions termed "slow" or "fast" or γ or γ' depending on the authors [10–12]. In a recent work Alegría and co-workers were able to isolate different components of the dielectric γ relaxation of PC taking advantage of the different extent to which these components are affected by stretching the sample [13,14]. Molecular orientation of PC obtained by stretching above the yield point at temperatures below the glass transition does not change the characteristic times or distributions of activation energies of the different components of the dielectric γ relaxation, but their intensity is reduced to a different extent [13,14]. For example, in a stretched sample with birefringence index $\Delta n=0.043$ (see later) the fast and main component of the dielectric relaxation spectra decreases by about 35% relative to an isotropic sample, whereas the slow component decreases only by ~14% (see Fig. 1). Moreover, the extent to which the intensity of the dielectric relaxation decreases is found to be proportional to the degree of structural orientation determined by birefringence measurements. Finally, dielectric relaxation experiments under hydrostatic pressure on PC show that an increase of pressure also modifies the relaxation spectra [15].

The comparison of the mean characteristic times for the different components of the dielectric γ relaxation in PC, which mainly follows the motion of the carbonate group, with those times extrapolated for the motions of PRs by NS shows that the slow component correlates well with the PR π-flip motion, whereas the fast component correlates with the additional ~3-Å jump of aromatic hydrogen atoms [6,14] (see arrows in Fig. 1). This coincidence supports the coupling between the motion of the carbonate group and the adjacent PR proposed in molecular dynamics simulation works. In line with these ideas, and as the decrease of the dielectric relaxation intensity is proportional to the degree of structural orientation, Alegría and co-workers explained the larger effect of stretching on the fast component in terms of motional hindrance. The better packing of polymer chains and the preferential orientation of PRs after stretching would pose higher difficulty to non-180° rotations than to π flips. Since the initial and final positions for a PR π flip are indistinguishable, an instantaneous fluctuation of the surrounding medium would be enough for the ring to flip before coming back to its initial configuration without disturbing the surrounding units permanently.

Stretching PC below the glass transition temperature causes densification, a lower concentration of free-volume holes [16,17], and some structural anisotropy in the polymer, although it still remains amorphous. X-ray-scattering measurements reveal that the main-peak position of stretched PC is shifted to higher angles relative to nonstretched PC, providing direct evidence of an increased packing density [14]. On the other hand, NMR studies of the structural modification of PC upon deformation indicate that PRs exhibit a tendency to orient parallel to each other and parallel to the deformation plane, while polymer chains tend to orient parallel to the deformation flow [18,19]. All these structural changes observed in stretched PC will play an important role in the model proposed, since as a result of increased steric hindrance and preferential orientation of PR, the ~90° rotation of some rings would be sterically impeded.

In this work we aim to prove at a molecular level the effect of stretching on PR dynamics by NS, a technique providing spatial information. In particular, we have studied the PR dynamics of stretched and isotropic fully protonated PC looking for preferential restriction on the ~3-Å jump of aromatic hydrogens, due to preferential orientation of the rings parallel to the stretching plane [18,19]. As shown in Fig. 8 of Ref. [6] (where the incoherent scattering of PR hydrogen atoms is selectively studied in a PC sample with deuterated methyl groups), the ~3-Å jump predominantly contributes at high values of the modulus of the momentum transfer Q (see Fig. 2) and at $T \gtrsim 300$ K, so we expect the quasielastic intensity of the stretched PC to be weaker than that of the nonstretched PC at $T \gtrsim 300$ K and high Q's.

III. EXPERIMENT

A. Samples

The PC samples used in this work were 0.175-mm-thick sheets supplied by Goodfellow CT301310 (the same used in Ref. [14]) due to the convenience of having ribbons of well-defined and reproducible dimensions for the stretching procedure. The molecular weight distribution of the polymer is $M_n=20.7$ kg mol^{-1} with polydispersity index equal to 2.66, as determined by means of gel permeation chromatography. The glass transition temperature measured by differential scanning calorimetry at the midpoint of the transition at 20 K/min is 420 K. To obtain uniaxially stretched samples, the specimens were placed in a circulating nitrogen atmosphere inside the heating chamber of a miniature material tester MINIMAT 2000 (Rheometrics Scientific). When the sample temperature was stabilized at 360 K, the sample (of ribbon shape, dimensions typically 8×30 mm^2) was

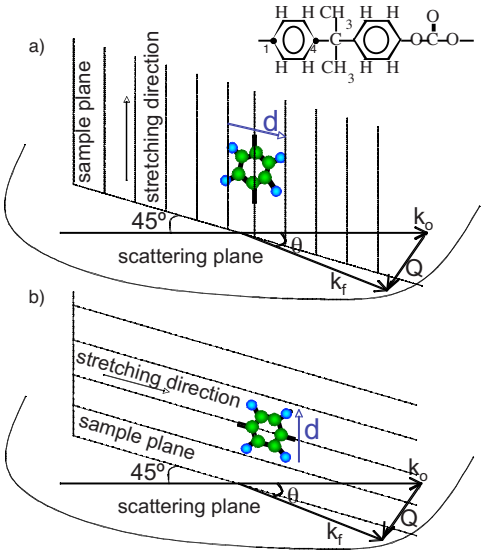

FIG. 2. (Color online) Sketch of the stretched$_\perp$ (a) and stretched$_\parallel$ (b) configurations.

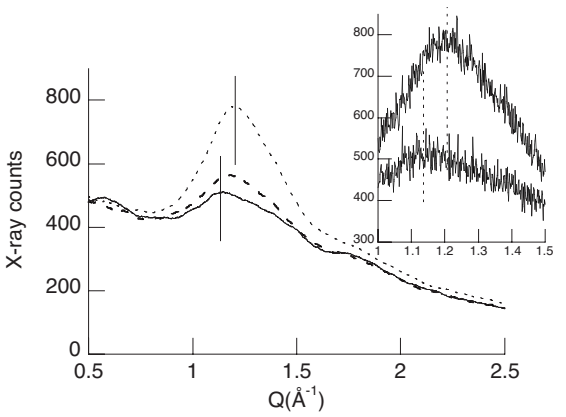

FIG. 3. XR spectra of stretched PC in three different sample diffractometer configurations: stretching direction parallel (solid line), perpendicular (dotted line), and at 45° (dashed line) relative to the scattering plane. Inset: raw data detail of the maxima of the parallel and perpendicular configurations.

stretched at a rate of 1.7 mm/s to achieve a draw ratio of 2.5, well above the yield point. Once the desired draw ratio was obtained, the specimen was rapidly cooled to room temperature. Only at the end of the cooling process was the mechanical stress maintaining the desired draw ratio removed. Sample thickness after stretching was between 0.11 and 0.12 mm. The sample anisotropy achieved by stretching was characterized by means of birefringence measurements using a prism coupler refractometer (Metricon 2010). The refractive index is isotropic before stretching, whereas it depends on the measuring direction after stretching, evidencing some degree of molecular orientation within the sample. The corresponding values of the birefringence index Δn (refractive index difference between two perpendicular directions in the sample) were in the range 0.046–0.052 for stretched samples and 0.001–0.003 for nonstretched ones. The anisotropy caused by stretching remains in time (at least months) at temperatures below and around room temperature. Short annealing (~10 min) at higher temperatures, however, produces an almost linear decrease of Δn with temperature, which does not depend much on the annealing time (tested up to 8 h). Samples lose the orientation and become completely isotropic when subjected to annealing at temperatures slightly above T_g. The equivalence between stretched PC subjected to deorientation treatment above T_g and isotropic samples was carefully checked by birefringence and DS measurements. Finally, to avoid any moisture absorption, all the samples were stored under dry nitrogen atmosphere before the subsequent experiments.

The anisotropy caused by stretching is also evident from the transmission x-ray diffraction of stretched PC. Measurements were done for three different sample-diffractometer configurations: sample stretching direction parallel, perpendicular, and at 45°, relative to the scattering plane. Data shown in Fig. 3 were smoothed in order to better appreciate the asymmetry of the stretched samples. The inset contains detail of the maxima of the parallel and perpendicular configurations showing the statistics of the raw data. A tendency for chains to anisotropically pack is inferred from the different position of the maxima for different configurations. The neutron coherent scattering of several BPA-PC samples with selective deuteration shows that the interchain carbon-carbon correlations contribute in a peak around 1.3 Å^{-1} [20] and agree with the position of the x-ray intensity maxima.

B. Neutron-scattering experiments

Quasielastic neutron scattering experiments were performed by means of the IN16 backscattering instrument at the Institute Laue Langevin in Grenoble. Two layers of four stretched PC ribbons (~10×15 mm^2 each) were used in a flat aluminum sample holder (3×4 cm^2) in order to obtain a neutron transmission close to 90%, optimizing the compromise between good statistics and reduced multiple-scattering contributions. The mean value of Δn for the ribbons in the aluminum container was 0.048. A wavelength of 6.271 Å was used, which leads to a Q range between 0.2 and 1.9 Å^{-1} and 0.5 μeV (half width at half maximum resolution). The energy window covered was ±15 μeV.

Both stretched and isotropic PC samples were isothermally measured in a 45° configuration (see Fig. 2). Taking into account the anisotropy produced by cold drawing, stretched samples were measured in two different arrangements: with the stretching direction parallel to the scattering plane (stretched$_\parallel$ from now on) and with the stretching direction perpendicular to the scattering plane (stretched$_\perp$ from now on); see Fig. 2. The stretched$_\parallel$ sample was measured at 10, 350, and 400 K, for 9, 9, and 6 h, respectively. While heating, additional 20-min spectra were obtained at intermediate temperatures. These spectra were used to determine the T dependence of the elastic intensity. After these measurements the stretched$_\parallel$ sample was isotropized *in situ* within the NS cryofurnace by an annealing treatment at 450 K for 75 min. The resulting isotropic sample was measured at 100, 200, 250, 300, 350, and 400 K for 1 h between 100 and 300 K and for 6 h at 350 and 400 K. Subsequent birefringence measurements confirmed the isotropy of this sample.

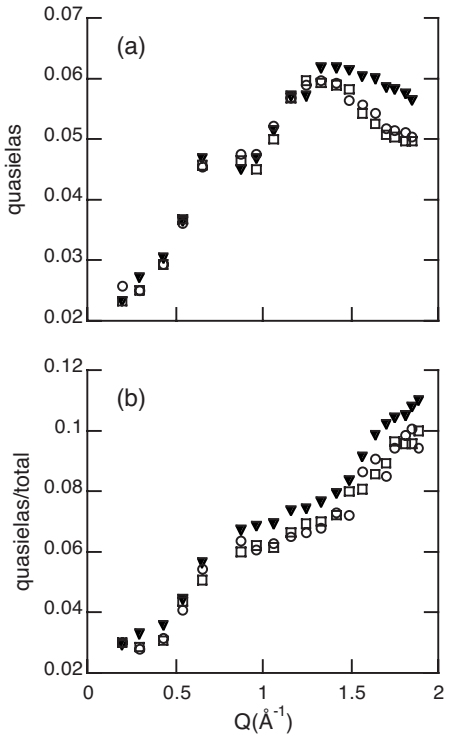

FIG. 4. (a) Integrated quasielastic intensity $a2(Q,T)$ as a function of Q and at 350 K for isotropic PC (triangles) and cold-drawn PC (squares and circles). (b) The data shown in (a) normalized to the total intensity in the IN16 window.

Finally, another stretched sample was measured at 350 and 400 K in the stretched$_{\perp}$ configuration for 9 and 6 h, respectively.

The neutron-scattered intensity consists of coherent and incoherent contributions weighed by the scattering cross sections of the different nuclei in the sample [21,22]. Hydrogen exhibits an extremely high value for the incoherent cross section and, therefore, incoherent scattering dominates the intensity measured in PC samples ($\sigma_{inc}/\sigma_{total}=0.9$). PC contains two types of hydrogen atoms: those in aromatic rings and those in methyl groups. As a result, the scattered intensity of fully protonated PC will consist of two main contributions coming from aromatic and methyl hydrogen atoms, respectively. After stretching we expect to have no changes in the signal of methyl hydrogens. As a result of stretching, our expectation is to find a decrease of less than about 20% in the total quasielastic intensity, in the limit of the usual statistics of a quasielastic spectra for molecular motions below T_g, which for typical IN16 spectra recorded for 8 h is approximately between 10% and 30%. The qualitative and quantitative dependence of the quasielastic broadening with temperature and Q can also be analyzed looking at the integrated quasielastic intensity in a given energy window. This representation of the data, which considerably reduces experimental noise, will be more suitable to emphasize variations of the quasielastic broadening with Q at a constant temperature and differences between the various samples.

The Q dependence of the quasielastic intensity integrated between 2 and 5 μeV, $a2(Q,T)$, is depicted in Fig. 4 for isotropic (triangles) and stretched (squares and circles) samples at 350 K. As can be seen, for this temperature both stretched and isotropic PC exhibit quasielastic broadening relative to the instrumental resolution, indicating the occurrence of aromatic, methyl, or aromatic and methyl hydrogen motions within the dynamic range of the instrument. Unexpectingly, the quasielastic intensity for parallel and perpendicular configurations do not differ appreciably. A similar behavior is found for the results at 400 K. It is worth noting in this figure that, in agreement with the expectations, a lower quasielastic intensity at high Q's is observed on the stretched specimens.

IV. MODELING

A. Isotropic PC

The analysis and modelization of isotropic PC neutron scattering were published in a previous communication [7]. As already mentioned in the experimental section, the NS signal of fully protonated PC consists of two main contributions coming from hydrogen atoms in methyl groups and PRs. The NS of isotropic PC is well described by 120° rotations of the methyl group and π flips, a 3-Å jump, and fast oscillations of PRs [6,7].

In the following, we will briefly describe the model used in Ref. [7] for isotropic PC, as it will be the starting point to describe the scattering of stretched PC samples. Neglecting the coherent contribution ($\sigma_{inc}/\sigma_{tot}=0.9$), the model scattering function describing the intensity scattered by isotropic PC is

$$I^{model}(Q,\omega) = D_{eff}[\sigma_{inc}^{H_{ar}} S_{H_{ar}}^{inc}(Q,\omega) + \sigma_{inc}^{H_{met}} S_{H_{met}}^{inc}(Q,\omega)], \tag{1}$$

with

$$S_{H_{ar}}^{inc}(Q,\omega) = \sum_k p_k S_{H_{ar}}^{k,inc}(Q,\omega), \tag{2}$$

$$S_{H_{met}}^{inc}(Q,\omega) = \sum_k p_k S_{H_{met}}^{k,inc}(Q,\omega), \tag{3}$$

$$S_{H_{ar}}^{k,inc}(Q,\omega) = S_{osc}^{k,inc}(Q,\omega) \otimes S_{3\ \text{Å}}^{k,inc}(Q,\omega) \otimes S_{flip}^{k,inc}(Q,\omega), \tag{4}$$

$$S_j^{k,inc}(Q,\omega) = A_j(Q)\delta(\omega) + [1 - A_j(Q)]\phi(\omega,\Gamma_j^k), \tag{5}$$

where j can be *osc*, 3-Å *jump, flip*, or H_{met} and D_{eff}, p_k, A_j, ϕ, and Γ_j^k represent, respectively, an effective Debye-Waller factor for times $\gtrsim 2$ ps, the weight of the distribution of characteristic times, the elastic incoherent structure factor (EISF) of the motion j [21], a Lorentzian function containing the dynamic information, and the characteristic rate of the j motion. The subscripts H_{ar} and H_{met} stand for aromatic and methyl group hydrogen atoms, respectively. The distribution of characteristic times p_k is parametrized in terms of a distribution of activation energies E_a via the Arrhenius relation for the T dependence of the characteristic times (rates), $\Gamma = 10^{13}\exp(-E_a/kT)$. In particular, an asymmetric function

TABLE I. Mean value $\langle E_a \rangle$ and width HWHM of the activation energy distributions for different motions in isotropic PC (MG =methyl group).

	MG_{rot}	PR_{osc}	$PR_{3\ Å}$	$PR_{\pi\ flip}$
$\langle E_a \rangle$ (eV)	0.22	0.20	0.32	0.41
HWHM (eV)	0.04	0.09	0.09	0.13

and a Gaussian distribution of activation energies were used for the oscillation and the 3-Å and flip motions, respectively (see [5–7,23] for more details). The mean value and the half width at half maximum (HWHM) of the distribution of activation energies for the different motions are shown in Table I.

The EISF function in Eq. (5) contains spatial information about the geometry of the motion [21,24], and its expression for the most general case is

$$A(Q) = |\langle \exp(i\vec{Q}\vec{r})\rangle|^2. \tag{6}$$

If the vector $\vec{d}=\vec{r}_i-\vec{r}_j$ going from the initial to the final position of the scattering center is randomly oriented relative to $\vec{Q}$ for different scattering centers, the resulting EISF for jumps between two positions is [21]

$$A(Q) = \frac{1}{2} + \frac{1}{2}\frac{\sin Qd}{Qd} \tag{7}$$

and, for jumps between three equidistant positions,

$$A(Q) = \frac{1}{3} + \frac{2}{3}\frac{\sin Qd}{Qd}. \tag{8}$$

During a π flip of a PR an aromatic hydrogen atom performs a jump between two equivalent positions at a distance 4.3 Å, and therefore the EISF for a π flip is the one defined in Eq. (7) with d=4.3 Å. The jump distance for the threefold rotation of methyl group hydrogens in Eq. (8) is d=1.78 Å.

B. Stretched PC

1. Anisotropy of stretched PC

Due to the anisotropy and preferential orientation caused by stretching, the vectors linking the initial and final positions of the scattering centers are no longer randomly oriented relative to $\vec{Q}$ in stretched PC. As a consequence, the EISF function in Eq. (7) (isotropic EISF from now on) is not valid anymore. We have calculated the EISF functions for some configurations of particular interest to this work according to the structural changes observed in stretched PC. In the following, we will use the label "anisotropic" for the EISF functions introduced below in order to distinguish them from the EISF defined in Eq. (7) for the isotropic case.

The anisotropic EISF function for a π-flip motion in the ideal particular case of the PR C1C4 axis oriented in the stretching direction, with PR planes parallel to the drawing plane, and in the stretched$_\perp$ configuration (see Fig. 2) is the following:

$$A_{flip}^{anis} = \frac{1}{2} + \frac{1}{2}\cos\left(\frac{ka}{\sqrt{2}}(1-\cos\theta-\sin\theta)\right), \tag{9}$$

where a is the jump distance of the aromatic hydrogen atom during a π flip—i.e., 4.3 Å—k is the modulus of the wave vector,[1] and θ is the scattering angle. The same function for the stretched$_\parallel$ case is one as the aromatic hydrogen displacement during a π flip for this configuration is perpendicular to the scattering plane. This fact is at the bottom of the comparison of the parallel and perpendicular configurations, as in the ideal case of the C1C4 axis perfectly aligned in the stretching direction, π-flip motion would not contribute to quasielastic intensity in the parallel configuration, while it would in the perpendicular one.

In order to calculate the anisotropic EISF for the ~3-Å jump, we need to know which is the exact nature of the motion making the initial and final positions of the aromatic hydrogen atoms to be 3 Å apart. According to the arguments presented in Sec. II we have modeled the ~3-Å jump as 90° rotations of PR. The anisotropic EISF function for 90° rotation of PRs in the ideal particular case of the PR C1C4 axis oriented in the stretching direction and PR planes either parallel or perpendicular to the drawing plane in the stretched$_\perp$ configuration would be

$$A_{rot}^{an} = \frac{1}{2} + \frac{1}{4}\{\cos[bk\sin\theta] + \cos[bk(1-\cos\theta)]\}, \tag{10}$$

b being the jump distance of the aromatic hydrogen during a 90° rotation. On the other hand, in the stretched$_\parallel$ configuration it would be equal to

$$A_{rot}^{an} = \frac{1}{2} + \frac{1}{2}\cos\left(\frac{bk}{2}\sin\theta + \frac{bk}{2}(1-\cos\theta)\right). \tag{11}$$

2. Quasielastic scattering of stretched PC

As we have already said, the model which has been proved to successfully describe the scattering of isotropic PC [Eq. (1)] will be the starting point to describe the NS of stretched PC. Among the different contributions to the scattered intensity in Eq. (1), it has been assumed that stretching does not affect the scattering of the methyl group due to the very local character of its motion [25]. On the other hand, according to DS results, we will assume throughout the calculations that the distributions of activation energies for the motions of PRs are the same in the isotropic and stretched PC. In addition, the EISF function for the fast oscillation motion of stretched PC will be taken isotropic for the sake of simplicity. The reason is that the oscillation motion at T =350 K and above is mainly centered in the microscopic time scale; thereby, its relative contribution to the quasielastic scattering in the mesoscopic time scale covered by the IN16 instrument is rather low.

In the following we will try to predict the effect on the scattering of PC of the orientation *only*, introducing in Eq. (2) the anisotropic EISF functions for π-flip and 90° rotation

[1] $k=|\vec{k}_0|\simeq|\vec{k}_f|$.

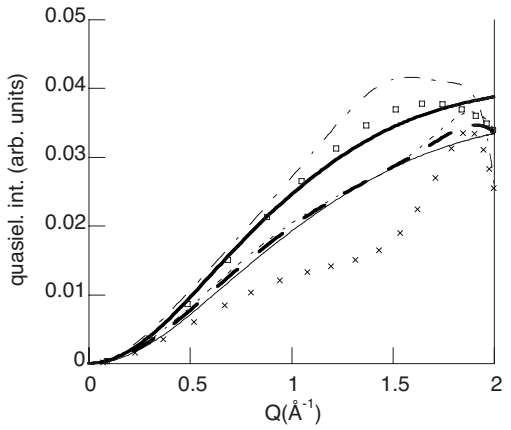

FIG. 5. Relative quasielastic intensity calculated in the stretched$_\perp$ configuration (D_{eff}=1) for (i) the isotropic case (thick solid line), (ii) an ideally anisotropic case (no motion reduction) (dash-dotted line), (iii) hindered 90° rotations (crosses), (iv) hindered 90° rotations for 35% of the rings (dotted line), (v) hindered π-flip motion for 35% of the rings (squares); (vi) hindered 90° rotations and π flips for 35% of the rings (thin solid line) and (vii) hindered 90° rotations for 35% and hindered π flips for 14% of the rings (dashed line).

motions of PRs presented above [from Eqs. (9)–(11)]. Figure 5 shows the quasielastic intensity, calculated with the model equation (1) and D_{eff}=1,[2] for (i) isotropic PC (thick solid line) and (ii) an ideal fully anisotropic case in the stretched$_\perp$ configuration (dot-dashed line), where all PR C1C4 axes would be oriented in the stretching direction and PR planes parallel to the drawing plane [EISF functions (9) and (10)]. As can be seen in the figure, the spatial anisotropy of the stretched sample alone—i.e., the different Q dependence of anisotropic EISF functions relative to isotropic ones—does not give an account of the decrease of the quasielastic intensity experimentally found.[3]

Provided the PR planes are preferentially located in the drawing plane, it naturally comes out that a PR ~90° rotation or any jump different from a π flip should be somehow hindered, or otherwise the mentioned preferred orientation would vanish. The quasielastic intensity predicted for such a case in which 90° rotations would be completely hindered [$S_{rot}^{k,inc}(Q,\omega)=\delta(\omega)$ in Eqs. (1)–(5) and crosses in Fig. 5] lies below the quasielastic intensity for the isotropic PC, in agreement with the experimental data. Apparently, calculations predict larger differences between the stretched and isotropic samples than those experimentally observed. Nevertheless, we have to bear in mind that the crosses in Fig. 5 represent an ideally anisotropic case in which all rings are perfectly aligned in a certain configuration, a situation improbable in reality. DS, birefringence, and NMR results indicate that there is no full molecular orientation, and therefore, it can be considered that only a fraction of the rings is affected by stretching. As a result, when modeling the scattered intensity of stretched PC we can assume that some fraction of the rings are not affected by stretching, whereas the remaining rings lie in a perfectly oriented state where 90° rotations are forbidden and where the PRs C1C4 axis and plane are parallel to the drawing direction and plane, respectively. In this framework, isotropic and anisotropic EISF functions will apply to the isotropic and oriented fraction of rings, respectively. The scattering function for such a model is

$$I^{model}(Q,\omega)=D_{eff}\Big(F(1-x)\sigma_{inc}^{H_{ar}}\delta(\omega)+Fx\sigma_{inc}^{H_{ar}}\sum_k p_k S_{H_{ar},2}^{k,inc}(Q,\omega)+(1-F)\sigma_{inc}^{H_{ar}}\sum_k p_k S_{H_{ar},3}^{k,inc}(Q,\omega)+\sigma_{inc}^{H_{met}}\sum_k p_k S_{H_{met}}^{k,inc}(Q,\omega)\Big), \quad (12)$$

where

$$S_{H_{ar},2}^{k,inc}(Q,\omega)=S_{osc}^{k,inc}(Q,\omega)\otimes S_{flip_a}^{k,inc}(Q,\omega), \quad (13)$$

$$S_{H_{ar},3}^{k,inc}(Q,\omega)=S_{osc}^{k,inc}(Q,\omega)\otimes S_{3\ \text{Å}}^{k,inc}(Q,\omega)\otimes S_{flip}^{k,inc}(Q,\omega), \quad (14)$$

and the $S_j^{k,inc}(Q,\omega)$ functions with j=*osc*, 3 Å *jump*, *flip*, *flip$_a$*, and H_{met} are defined as in Eq. (5), the subscript *flip$_a$* in $S_{flip_a}^{k,inc}(Q,\omega)$ means that the EISF for flips in this function is the anisotropic one [Eq. (9) for stretched$_\perp$ and EISF=1 for stretched$_\parallel$ configurations, respectively], F represents the fraction of oriented PRs, and x is the fraction of oriented PRs which can flip and oscillate.

The idea of PR planes preferentially oriented in the drawing plane hindering ~90° rotations is quite intuitive. However, the way in which stretch-induced anisotropy and densification affect π-flip dynamics is not straightforward. In principle, it is reasonable to think that there will be some effect, but a complete arrest of this motion is not so clear, as an instantaneous fluctuation could be enough for the ring to flip before coming back to its initial configuration [26]. Concerning fast oscillations, as we have said before, its contribution to the time scale of the IN16 instrument at $T\geqslant 350$ K is very small. Thereby, for the sake of simplicity we will assume the fraction of PRs that as a result of stretching cannot flip and cannot oscillate to be the same.

For example, for F=0.35 and x=0.6 (compatible with DS results) the reduction of the quasielastic intensity obtained for the stretched sample (dashed line in Fig. 5) is close to the experimental behavior (see Fig. 4). Also shown in Fig. 5 are the calculated quasielastic intensities for F=0.35 and x=1 (dotted line) and F=0.35 and x=0 (solid thin line). From the

[2]This would qualitatively be as looking at the quasielastic intensity normalized to the total intensity—i.e., to the relative quasielastic intensity—and therefore, results can be compared with the normalized experimental intensities shown in Fig. 4(b).

[3]Convolution of the model scattering function with the experimental resolution introduces some degree of "experimental noise" in the modeled intensities as a function of Q because instrumental resolution is Q dependent. Therefore, a Q-independent average model resolution function representative of the IN16 instrument resolution was used for the curves shown in Fig. 5.

closeness of these last three curves (solid thin, dotted, and dashed lines), it is clear that it is difficult to clearly establish the fraction of oriented PRs performing π flips within the experimental accuracy of the NS data. Nevertheless, these to some extent not so different situations can be clearly distinguished from, for example, a picture in which π flips but not 90° rotations would be forbidden for 35% of the oriented rings (squares). Therefore, though we cannot accurately determine the fraction of PRs with arrested π-flip motion from the NS data, the above analysis shows that a substantial reduction of 3-Å jumps is needed to explain the decrease of the quasielastic intensity observed after stretching PC, in agreement with (i) the existence of preferentially oriented PRs after cold deformation found by NMR and (ii) the observed dielectric γ relaxation of PC and its interpretation for cold-stretched samples. It is worth noting that as long as the ~3-Å jump of aromatic hydrogen atoms is considered to be hindered in the oriented state, the exact nature of the motion—i.e., if it is a consequence of a 90° rotation of PR or not—is not relevant anymore, as its contribution to Eq. (12) will be only in the "isotropic" part.

V. DATA ANALYSIS AND DISCUSSION

Applying the model equation (12), the fractions F and x which best describe the experimental NS data were computed. The modeled integrated intensities were calculated by convolution of Eq. (12) with the experimental Q-dependent resolution. Figures 6(a)–6(c) show the experimental (symbols) and calculated (solid lines) quasielastic integrated intensities normalized to the total intensity of the spectra for isotropic, stretched$_{\parallel}$, and stretched$_{\perp}$, samples at 350 K with $F=0.40$ and $x=0.75$ and at 400 K with $F=0.25$ and $x=0.80$. The calculation of the normalized quasielastic intensity has the advantage that no D_{eff} is needed to compute it. Thus, the so-obtained curves would be qualitatively equivalent to those shown in Fig. 5, which were calculated for $D_{eff}=1$. Taking into account that all the parameters were fixed except F and x, the agreement between the calculated and experimental data is very good. In order to calculate the absolute quasielastic and elastic intensities shown in Figs. 6(d)–6(f), the D_{eff} was taken equal to that obtained for a PC sample with deuterated methyl groups in Ref. [6]. The very similar mean-square displacements found below the onset of methyl group rotation at temperatures ~200–250 K for that sample and for the fully protonated PC support this choice as a good approximation. It is again worth noting the excellent agreement obtained between the calculated and measured intensities. The slight deviations around 1.25 Å^{-1} are due to the Q modulation of the intensity caused by coherent contributions, which were not taken into account in the model.

The agreement with experimental data is good for both parallel and perpendicular configurations. This is not trivial, since the calculations for these two configurations include different EISF functions balanced by the same dynamical $\phi(\omega,\Gamma)$ functions. The model thus reproduces the unexpected similarity found in the quasielastic intensity of the parallel and perpendicular configurations. This similarity, although counterintuitive, is predicted by equations and is, after all, a natural consequence of the balance of the different contributions to the quasielastic intensity.

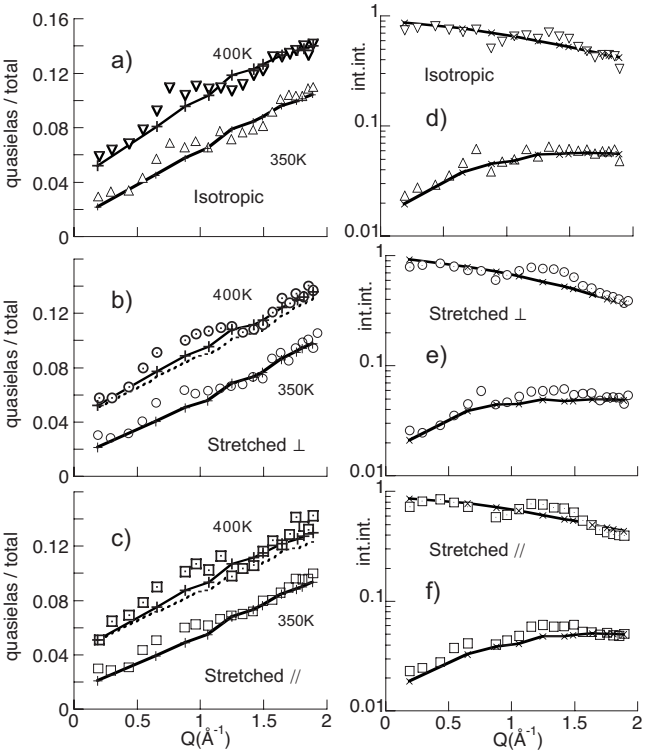

FIG. 6. (a), (b), and (c) Quasielastic intensity relative to total intensity for isotropic, stretched$_{\perp}$, and stretched$_{\parallel}$ samples at 350 and 400 K; data at 400 K have been shifted 0.03 in the y axis for clarity. (d), (e), and (f) Integrated elastic (down triangles, dotted circles, and dotted squares) and quasielastic intensities (up triangles, circles, and squares) for the isotropic, stretched$_{\perp}$, and stretched$_{\parallel}$ samples at 350 K, respectively. Crosses linked by solid lines represent the same magnitudes calculated with the model [Eq. (12)] with (F,x) equal to (0.40,0.75) at 350 K and (0.25,0.80) at 400 K, respectively. Dotted lines represent the model with (0.40,0.75) at 400 K.

The uncertainty in the (F,x) pair values is rather large, between (0.35,0.6) and (0.55,1) at 350 K and between (0.25,0.75) and (0.35,1) at 400 K. F and x are highly coupled so that pairs providing a good description of the data have the F/x ratio nearly constant. The fraction of PRs with arrested ~3-Å jumps obtained by NS is in semiquantitative agreement with the degree of orientation measured by birefringence, $\Delta n/\Delta n_{cryst}$ [27], for each sample (see Table II). The lower F value obtained at 400 K is not surprising if we take into account the decrease of anisotropy in stretched samples as temperature increases. Subsequent measurements showed that the birefringence of the sample had decreased from 0.048 to 0.029 as a result of the thermal history of NS experiments (data acquisition at 400 K lasted 6 h). Finally, the agreement between NS and DS results in stretched PC samples is also very good. The reduction after stretching of the dielectric γ-relaxation fast component was 35% and that of the slow component was 14%, which lie within the same (F,x) range determined by NS (see Table II).

TABLE II. F: the fraction of PRs in a preferentially oriented state—i.e., with arrested ~3-Å jumps. x: the fraction of flipping PRs within the preferentially oriented state. $F^*(1-x)$: The total fraction of rings with arrested π-flip motion.

	NS_{350}	NS_{400}	DS[a]
F	0.35–0.55	0.25–0.35	0.35
x	0.6–1.0	0.75–1	0.86
$F^*(1-x)$	0–0.22	0–0.09	0.14
$\frac{\Delta n}{\Delta n_{cryst}}$[b]	0.30	0.18	

[a]Dielectric spectroscopy between 120 and 300 K.
[b]Birefringence values relative to those of the fully crystalline state at 350 and 400 K.

VI. CONCLUSIONS

Quasielastic NS measurements of stretched and isotropic PC have been performed. The spectra from stretched and isotropic samples are different, the quasielastic broadening being larger for the isotropic sample. The scattered intensity in the isotropic sample can be well described by a model which considers π flips, a ~3-Å jump, and fast oscillations of PRs. The difference between isotropic and stretched PC can be well accounted for by considering that as a result of stretching preferentially oriented PRs have the ~3-Å jump sterically hindered. In contrast, only between 0 and 40% of preferentially oriented PRs lose the ability to flip at $T \geqslant 350$ K.

The fraction of PRs for which ~3-Å jump and π-flip motions are hindered obtained from NS data analysis agree well with the reduction percentages observed for the two components of the dielectric γ relaxation of stretched PC. These results support once again the coupled motion between carbonate group and PRs and the molecular origin of the dielectric relaxations as due to the concerted motion of these two moieties. Moreover, the microscopic spatial information (Q dependence) of the stretched PC relative to the isotropic one is fully compatible with a hindered ~3-Å jump of PR produced by a preferential orientation of PR planes parallel to the stretching plane. Likewise, the reduction of the ~3-Å jump of PR (and dielectric fast component) is in agreement with the degree of anisotropy measured by birefringence. The overall picture would provide another argument for the interpretation of the ~3-Å jump of aromatic hydrogen atoms as ~90° rotations of PR.

ACKNOWLEDGMENTS

This research project has been supported by the European Commission NoE SoftComp, Contract No. NMP3-CT-2004-502235, Project Nos. MAT2007-63681 and IT-436-07 (G.V.), the Spanish Ministerio de Educacion y Ciencia (Grant No. CSD2006-53), the Consejo Superior de Investigaciones Científicas, and the Donostia International Physics Center. O.M. also acknowledges grants from the Basque Government and the University of the Basque Country.

[1] M. Wehrle, G. P. Hellmann, and H. W. Spiess, Colloid Polym. Sci. **265**, 815 (1987).
[2] M. T. Hansen, C. Boeffel, and H. W. Spiess, Colloid Polym. Sci. **271**, 446 (1993).
[3] M. T. Hansen, A. S. Kulik, K. O. Prins, and H. W. Spiess, Polymer **33**, 2231 (1992).
[4] I. Quintana, A. Arbe, J. Colmenero, and B. Frick, Macromolecules **38**, 3999 (2005).
[5] S. Arrese-Igor, A. Arbe, A. Alegría, J. Colmenero, and B. Frick, J. Chem. Phys. **120**, 423 (2004).
[6] S. Arrese-Igor, A. Arbe, A. Alegría, J. Colmenero, and B. Frick, J. Chem. Phys. **123**, 014907 (2005).
[7] S. Arrese-Igor, A. Arbe, A. Alegría, J. Colmenero, and B. Frick, J. Non-Cryst. Solids **352**, 5072 (2006).
[8] J. H. Shih and C. L. Chen, Macromolecules **28**, 4509 (1995).
[9] C. F. Fan, T. Çagin, W. Shi, and K. A. Smith, Macromol. Theory Simul. **6**, 83 (1997).
[10] N. G. McCrum, B. E. Read, and G. Williams, *Anelastic and Dielectric Effects in Polymeric Solids* (Dover, New York, 1967).
[11] D. C. Watts and E. P. Perry, Polymer **19**, 248 (1978).
[12] A. S. Merenga, C. M. Papadakis, F. Kremer, J. Liu, and A. F. Yee, Macromolecules **34**, 76 (2001).
[13] O. Mitxelena, J. Colmenero, and A. Alegría, J. Non-Cryst. Solids **351**, 2652 (2005).
[14] A. Alegría, O. Mitxelena, and J. Colmenero, Macromolecules **39**, 2691 (2006).
[15] A. Alegría, S. Arrese-Igor, O. Mitxelena, and J. Colmenero, J. Non-Cryst. Solids **353**, 4262 (2007).
[16] S. S. E. Ito and K. Sawamura, Colloid Polym. Sci. **253**, 480 (1975).
[17] D. Cangialosi, M. Wübbenhorst, H. Shcut, and A. van Veen, J. Chem. Phys. **122**, 064702 (2005).
[18] M. Utz, A. S. Atallah, P. Robur, A. H. Widmann, R. R. Ernst, and U. W. Suter, Macromolecules **32**, 6191 (1999).
[19] M. Utz, P. Robyr, and U. W. Suter, Macromolecules **33**, 6808 (2000).
[20] J. Eilhard, A. Zirkel, W. Tschöp, O. Hahn, K. Kremer, O. Schärpf, D. Richter, and U. Buchenau, J. Chem. Phys. **110**, 1819 (1999).
[21] M. Bée, *Quasielastic Neutron Scattering* (Hilger, Bristol, 1988).
[22] S. W. Lovesey, *Theory of Neutron Scattering from Condensed Matter* (Oxford University Press, Oxford, 1987).
[23] S. Arrese-Igor, A. Arbe, A. Alegría, J. Colmenero, and B. Frick, J. Chem. Phys. **122**, 049902 (2005).
[24] M. Bée, Physica B **182**, 323 (1992).
[25] F. Alvarez, A. Alegría, j. Colmenero, T. M. Nicholson, and G. R. Davies, Macromolecules **33**, 8077 (2000).
[26] D. R. Whitney and R. Yaris, Macromolecules **30**, 1741 (1997).
[27] R. S. Stein and G. L. Wilkes, in *Structure and Properties of Oriented Polymers*, edited by I. M. Ward (Wiley, New York, 1975), p. 150.